Single Wall Carbon Nanotube Dispersion and Exfoliation in Polymers

Tetsuya Uchida,[1] Satish Kumar[2]

[1]*Faculty of Engineering, Okayama University, Okayama, 700-8530, Japan*
[2]*School of Polymer, Textile and Fiber Engineering, Georgia Institute of Technology, Atlanta, Georgia 30332*

Received 23 November 2004; accepted 6 March 2005
DOI 10.1002/app.22203
Published online in Wiley InterScience (www.interscience.wiley.com).

ABSTRACT: Dispersion and exfoliation of single wall carbon nanotubes (SWNTs) have been studied in poly(acrylonitrile) (PAN), poly(*p*-phenylene benzobisoxazole) (PBO) solutions, and composite fibers using transmission electron microscopy. As a result of polymer assisted dispersion and exfoliation, the average SWNT bundle diameter in SWNT/PAN (5/95) was 11 nm, while the average diameter for the pristine SWNT bundles was about 30 nm. High resolution TEM of SWNT/PBO (10/90) composite fibers did not reveal the presence of SWNT aggregates or bundles, suggesting SWNT exfoliation as individuals. On the other hand, both oriented and unoriented nanotube bundles have been observed in SWNT/PBO samples containing 15 wt % nanotubes. Carbon nanotubes are 10^5 times more radiation resistant than flexible polymers such as polyethylene, and 10^3 times more resistant than highly radiation resistant polymers such as PBO. Therefore in the high resolution TEM study of nanotube/polymer composites, nanotubes can be observed long after the polymer has been damaged by electron radiation. J Appl Polym Sci 98: 985–989, 2005

Key words: carbon nanotube; electron beam irradiation; nanocomposite; PAN; TEM

INTRODUCTION

The discovery of single wall carbon nanotubes[1,2] is inspiring the development of new high performance materials. SWNTs possess a unique combination of mechanical, electrical, and thermal properties, and density.[3–7] The carbon nanotube aspect ratio can typically be in the range of 10^4–10^5 and have high tensile strength (37 GPa), tensile modulus (640 GPa to 1 TPa),[8–11] and low density (as low as 1.3 g/cm^3). However, there are many obstacles to processing carbon nanotube based polymer composites. Metal catalyst particles of about 4 nm in diameter can typically be 30 to 40 wt % of the total weight in the carbon nanotube as an impurity, and it must be removed[12–14] for most applications. For composite applications, purified tubes should be dispersed in polymer and other type matrices. Exfoliation[15] of nanotubes as individuals in the matrix is important for maximizing the translation of nanotube properties in the composite.

Significant research efforts are being devoted towards dispersing and exfoliating nanotubes in various matrices.[16] Sonication and *in situ* polymerization have been effectively used for nanotube dispersion and exfoliation.[17,18] High resolution transmission electron microscopy study of SWNT dispersion and exfoliation in polyacrylonitrile (PAN) and in poly(*p*-phenylene benzobisoxazole) (PBO) have been carried out and are reported in this paper.

EXPERIMENTAL

HiPCO SWNTs (average diameter about 1 nm)[19] were purified by heating at 250°C in moist air to convert the iron clusters to iron oxides, followed by their removal by continuous (soxhlet) extraction in HCl. The residual iron content of the purified SWNTs dispersed in PBO was about 1 wt %, while the residual iron content of SWNTs used in PAN was about 7 wt %. The residual iron content is based on thermogravimetric analysis (TGA) when the nanotubes were heated in air at 10°C/min in a TA instruments thermogravimetric analyzer, TGA 2950.

The polyacrylonitrile-*co*-methyl acrylate (copolymer molar ratio 90 : 10, molecular weight 100,000 g/mol) was obtained from Sigma Aldrich and used as received. SWNT/PAN composite fibers were prepared by solution processing in dimethyl formamide (DMF).[17] Properties of the control PAN and SWNT/PAN composite fibers are listed in Table I. The SWNT/PBO composite dope was prepared by *in situ* polycondensation of bis(aminophenol) and terepthalic acid, and the fibers spun using dry-jet wet spinning.[18] Spun fibers were continuously washed in water for 1 week, vacuum dried at 80°C for 12 h, and subse-

Correspondence to: S. Kumar (satish.kumar@ptfe.gatech.edu).

TABLE I
Mechanical Properties of PAN and SWNT/PAN Composite Fibers[17]

SWNT (wt %)	Tensile modulus (GPa)	Tensile strength (GPa)
0	7.9 ± 0.4	0.23 ± 0.03
5	14.2 ± 0.6	0.36 ± 0.02

quently heat-treated in nitrogen under tension (40 MPa) for 2 min at 400°C. Mechanical properties of SWNT/PBO fibers are listed in Table II. All tensile testing was done on 2.54 cm gauge length single filaments. Typically, 25 fibers were tested in each case.

Thin specimens for transmission electron microscopy were prepared directly from the spinning dope as well as from the composite fibers. SWNT/PAN/DMF spinning dope was directly spread on the holey carbon grid, and then the solvent was evaporated at room temperature. Thin specimens from the composite fibers were prepared using the detachment method.[20,21] The composite fibers were placed on the adhesive collodion surface. After coagulation of the collodion film, the fibers were detached, and consequently thin split sections of fiber remained on the collodion surface. The collodion film containing thin fiber sections was placed on the holly carbon grid and rinsed with amyl acetate, resulting in thin specimens without collodion on the TEM grid. SWNT/PBO spinning dope coagulated in water was used to make thin specimens in a manner similar to the SWNT/PBO fiber. Bright field images were recorded on Kodak Microscope Film (SO163) using a high-resolution transmission electron microscope (JEM 4000EX) operated at 300 kV.

RESULTS AND DISCUSSION

Transmission electron micrographs show SWNT bundles as well as metal particles in the unpurified sample [Fig. 1(a)]. A comparison of Figure 1(a–b) also shows that most metal particles have been removed in the purification process. This TEM observation is consistent with the TGA analysis (Fig. 2), which shows that the residual weight of the purified samples on heating to above 800°C in air is much less than the residual

TABLE II
Mechanical Properties of PBO and SWNT/PBO Composite Fibers

SWNT (wt %)	Tensile modulus (GPa)	Tensile strength (GPa)
0	138 ± 20	2.6 ± 0.3
10	167 ± 15	4.2 ± 0.5
15	108 ± 10	2.0 ± 0.5

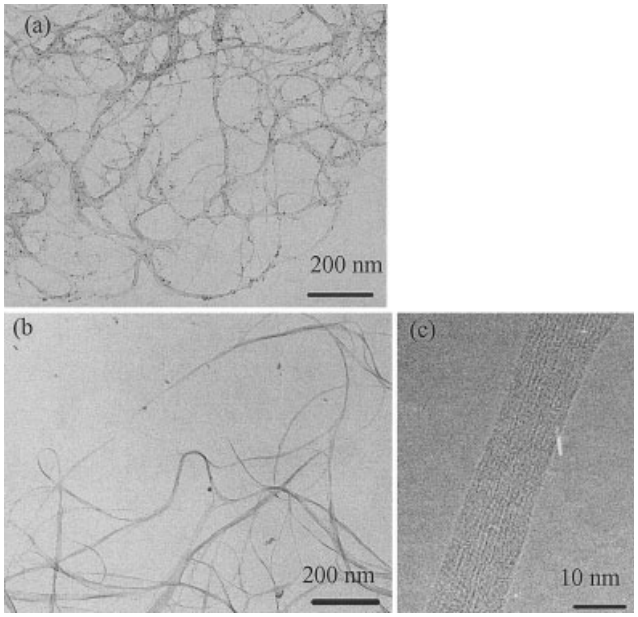

Figure 1 Transmission electron micrographs of (a) unpurified, and (b and c) purified SWNT bundles.

weight for the unpurified sample. The weight gain in the 200 to 350°C range [Fig. 2(a)] in the unpurified samples is a result of oxidation of the catalytic impurity (Fe). The residual weight in Figure 2 represents the weight of iron oxide. In the case of the composite fiber made with the unpurified SWNTs, metallic particles remain in the SWNT bundles, as confirmed by high resolution transmission electron microscopy (Fig. 3); and the tensile strength of the SWNT/PBZT composite fiber containing SWNT catalytic impurity did not show significant improvement over the control fiber.[22] Therefore, the purified SWNTs were used for the following study. The average diameter of the bundle of purified SWNTs based on extensive TEM studies was determined to be 30 ± 15 nm. High resolution electron micrographs [Fig. 1(c)] and X-ray diffraction

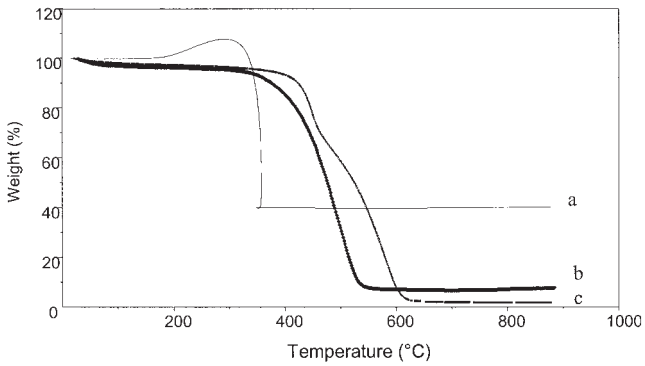

Figure 2 Thermogravimetric analysis of (a) unpurified, (b) purified, and (c) ultra-purified SWNTs in air at a heating rate of 10°C/min.

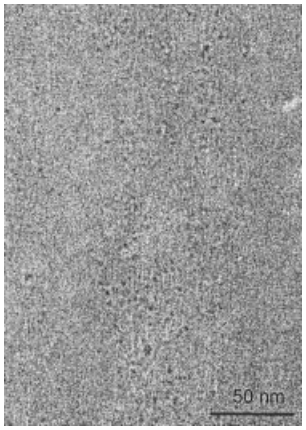

Figure 3 Transmission electron micrographs of unpurified SWNT/PBZT composite fiber.

of the purified SWNT bundle show the lattice image and diffraction peaks, indicating order in the SWNT bundle.[23,24] The data in Table III show that the threshold energy for ballistic damage in SWNTs is at least 10^5 times the total end-point dose for radiation sensitive polymers such as polyethylene and more than three orders of magnitude the end-point dose for most radiation resistant polymers such as PBO.[25–27] Due to this difference between the electron beam sensitivities of carbon nanotubes and polymers, under TEM observation the SWNT structure is more stable than the polymer matrix and, therefore, lattice image of SWNT bundles can be observed long after the lattice image of the polymer matrix has been damaged due to radiation.

Mechanical properties of the SWNT/PAN composite fibers are higher than those of the control PAN fiber (Table I). Lattice images of SWNT bundles can be observed in the PAN matrix [Fig. 4(a)]. Individual SWNTs have also been occasionally observed in the PAN matrix [Figs. 4(a) and 4(c)]. Based on TEM observations, the diameter distribution of SWNT bundles in the SWNT/PAN (5/95) composite measured from many images is given in Figure 5 and has been compared to the diameter distribution of the purified SWNT bundles. In the SWNT/PAN composite, the average rope diameter was 11 ± 6 nm. By comparison, the average diameter of purified SWNT bundles sonicated in methanol for 10 min was 30 ± 15 nm. This is a result of polymer assisted dispersion and partial exfoliation. Calculated tensile modulus of the composite fiber was found to be consistent with these SWNT bundle diameter measurements.[17] The average rope diameter in the spun and drawn fiber may be lower than in the dope, as the fiber spinning and drawing process may further exfoliate the nanotube bundles.

TABLE III
Critical Electron Dose for SWNT, PBO, and polyethylene

	($e^- nm^{-2}$)
SWNT at 200kV [1][27]	3.5×10^8
PBO at 200kV [2][26]	5.0×10^4
Polyethylene at 200kV [2][26]	9.0×10^2

[1]Threshold energy for ballistic damage in SWNTs.
[2]Total end-point dose (TEPD).

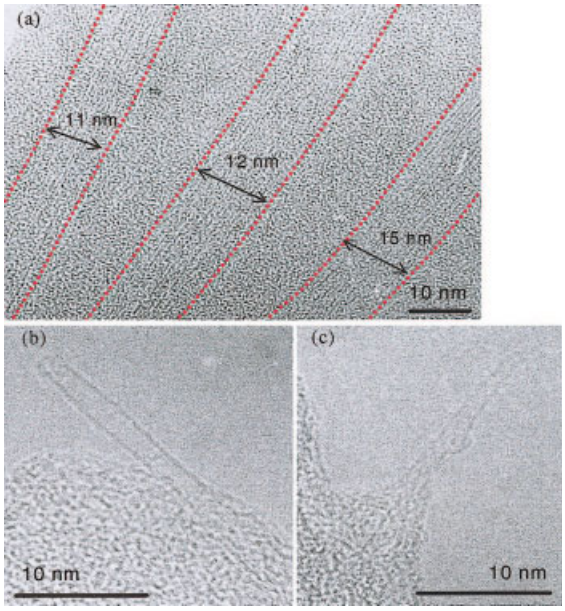

Figure 4 Transmission electron micrographs of SWNT bundles (a) and individual SWNTs (b and c) in the SWNT/PAN (5/95) composite. [Color figure can be viewed in the online issue, which is available at www.interscience.wiley.com.]

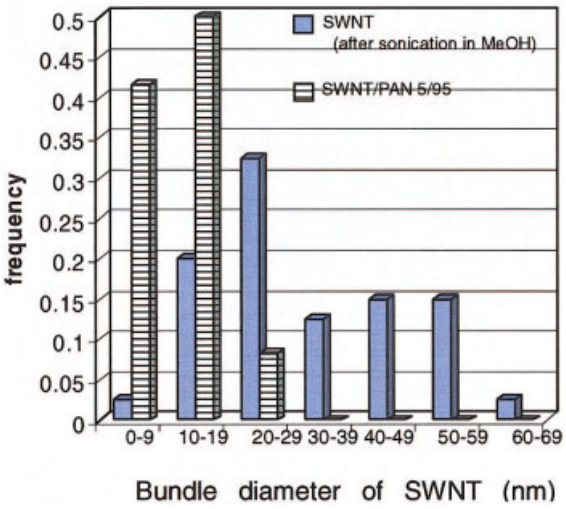

Figure 5 Diameter distributions of pristine SWNT bundles and SWNT bundles in SWNT/PAN (5/95). [Color figure can be viewed in the online issue, which is available at www.interscience.wiley.com.]

Individual SWNTs or SWNT bundles were not observed in the SWNT/PBO (10/90) fiber (Fig. 6); however, the PBO lattice image could be observed. This suggests that experimental conditions and the electron irradiation dosage level were quite low, and therefore SWNTs should not be damaged under these conditions. The question is why SWNTs could not be observed in the SWNT/PBO (10/90) composite fiber. The average diameter of SWNTs used in this study is about 1 nm. On the other hand, from the imaging contrast, we can say that the thickness of the SWNT/PBO (10/90) fiber specimen used for TEM observation is at least several tens of nanometers. Therefore, the TEM image is dominated by the polymer matrix, making the observation of individual SWNTs difficult. Further support for this argument comes from Figure 4(b) and 4(c), where individual SWNTs covered by the PAN matrix cannot be observed under these TEM observation conditions, and only that part of the SWNT not covered by the polymer matrix could be observed and imaged. We conclude that SWNTs in the SWNT/PBO (10/90) composite fiber exist as individual tubes in the PBO matrix. The presence of SWNT in this fiber was indeed confirmed by Raman spectroscopy.[18] Unoriented and oriented SWNT bundles were observed in PBO containing 15 wt % carbon nanotubes and exhibiting low tensile strength. Nanotube aggregates, of several hundred nanometer dimension, were randomly dispersed in SWNT/PBO (15/85) dope [Fig. 7(a)]. Figure 7(b) shows the presence of SWNT bundles of 20–50 nm diameter aligned nearly parallel to the fiber axis. Improved tensile strength PBO fibers were made with ultra-pure nanotubes (catalytic impurity less than 1 wt %, Fig. 2(c) fully exfoliated in the PBO matrix. Improvements in tensile strength were not observed when the nanotube impurity level was 10 wt % or when nanotubes were not fully exfoliated in the matrix.

CONCLUSIONS

The SWNT bundle diameter in the SWNT/PAN (5/95) composite was about 11 nm, while the average diameter of the pristine SWNT bundles was about 30 nm. Some individual SWNTs were also observed in the SWNT/PAN composite. SWNT bundles were not observed in the SWNT/PBO (10/90) composite fiber exhibiting high tensile strength, while SWNT/PBO (15/85) dope as well as fibers showed the presence of nanotube bundles and did not result in improved strength PBO fiber. In highly ordered fibers such as PBO, catalyst particles are detrimental to tensile strength. Current production methods yield SWNTs with a diameter distribution, for example, in the typical HiPCO run, more than 90% of the tubes are in the 0.7 to 1.4 nm diameter range. Such a broad diameter distribution results in low shear modulus, making exfoliation necessary. Production of uniform diameter tubes of a given chirality is expected to result in higher shear modulus, making the SWNT bundle exfoliation requirement less critical.

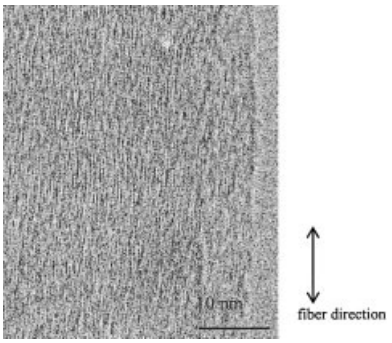

Figure 6 Transmission electron micrograph of heat-treated SWNT/PBO (10/90) fiber.

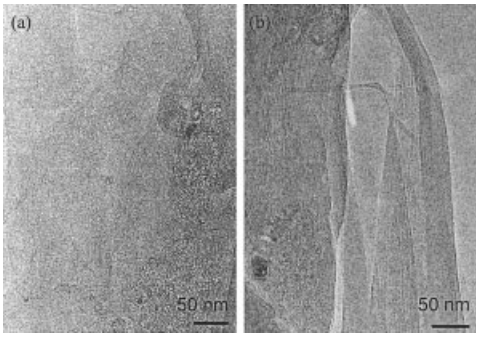

Figure 7 Transmission electron micrographs of (a) dope and (b) heat-treated fiber for SWNT/PBO (15/85).

This work was supported by Air Force Office of Scientific Research (F49620–03-1–0124) and the Office of Naval Research (N00014–01-1–0657). SWNT/PBO polymerization was carried out by Thuy Dang at the U. S. Air Force Research Laboratory. SWNT/PBO fibers were processed by Xiefei Zhang, and SWNT/PBO fibers were processed by Dr. T. V. Sreekumar.

References

1. Iijima, S.; Ichihashi, T. Nature 1993, 363, 603.
2. Bethune, D. S.; Kiang, C. H.; DeVries, M. S.; Gorman, G.; Savoy, R.; Beyers, R. Nature 1993, 363, 605.
3. Yakobson, B. I.; Smalley, R. E. Am Sci 1997, 85, 324.
4. Treacy, M. M. J.; Ebbesen T. W.; Gibson, J. M. Nature (London) 1996, 381, 678.
5. Wong, E. W.; Sheehan, P. E.; Lieber, C. M. Science 1971 1997, 277.
6. Poncharal, P.; Wang, Z. L.; Ugarte, D.; De Heer, W. A. Science 1999, 283, 1513.
7. Baughman, R. H.; Zakhidov, A. A.; De Heer, W. A. Science 2002, 297, 787.
8. Lu, J. P. Phys Rev Lett 1997, 79, 1297.
9. Gao, G.-H.; Cagin, T.; Goddard, W. A. Nanotechnology 1998, 9, 184.
10. Sinnott, S. B.; Shenderova, O. A.; White, C. T.; Brenner, D. W. Carbon 1998, 36, 1.

11. Popov, V. N.; Van Doren, V. E.; Balkanski, M. Solid State Commun 2000, 114, 395.
12. Strong, K. L.; Anderson, D. P.; Lafdi, K.; Kuhm, J. N. Carbon 2003, 41, 1477.
13. Dillon, A. C.; Gennet, T.; Jones, K. M.; Alleman, J. L.; Parilla, P. A.; Heben, M. J. Adv Mater 1999, 11, 1354.
14. Chiang, I. W.; Brinson, B. E.; Smalley, R. E.; Margrave, J. L.; Huage, P. H. J Phys Chem B 2001, 105, 1157.
15. Liu, T.; Kumar, S. Nano Letters 2003, 3, 647.
16. Sabba, Y.; Thomas, E. L. Macromolecules 2004, 37, 4815.
17. Sreekumar, T. V.; Liu, T.; Min, B. G.; Guo, H.; Kumar, S.; Hauge, R. H.; Smalley, R. E. Adv Mater 2004, 16, 58.
18. Kumar, S.; Dang, T. D.; Arnold, F. E.; Bhattacharyya, A. R.; Min, B. G.; Zhang, X.; Vaia, R. A.; Park, C.; Adams, W. W.; Hauge, R. H.; Smalley, R. E.; Ramesh, S.; Willis, P.A. Macromolecules 2002, 35, 9039.
19. Nikolaev, P.; Bronikowski, M. J.; Bradley, R. K; Rohmund, F.; Colbert, D. T; Smith, K. A.; Smalley, R. E. Chem Phys Lett 1999, 313, 91.
20. Shimamura, K.; Minter, J. R; Thomas, E. L. J Mater Sci Lett 1983, 18, 54.
21. Adams, W. W.; Kumar, S.; Martin, D. C.; Shimamura, K. Polym Commun 1989, 30, 285.
22. Unpublished data of authors.
23. Thess, A.; Lee, R.; Nikolaev, P.; Dai, H.; Petit, P.; Robert, J.; Xu, C.; Lee, Y. H.; Kim, S. G.; Rinzler, A. G.; Colbert, D. T.; Scuseria, G.; Tománek, D.; Fischer, J. E.; Smalley, R. E. Science 1996, 273, 483.
24. Zhang, X.; Sreekumar, T. V.; Liu, T.; Kumar, S. J Phys Chem B 2004, 108, 16435.
25. Kumar, S.; Adams, W. W. Polymer 1990, 31, 15.
26. Martin, D. C.; Thomas, E. L. Polymer 1995, 36, 1743.
27. Smith, B. W.; Luzzi, D. E. J Appl Phys 2001, 90, 3509.